AGU ADVANCING EARTH AND SPACE SCIENCE

Water Resources Research

RESEARCH ARTICLE
10.1029/2021WR030406

Contextualizing Inflow and Infiltration Within the Streamflow Regime of Urban Watersheds

Luke A. Pangle[1], Jeremy E. Diem[1], Richard Milligan[1], Ellis Adams[2], and Allison Murray[1]

[1]Department of Geosciences, Georgia State University, Atlanta, GA, USA, [2]Keough School of Global Affairs, University of Notre Dame, Notre Dame, IN, USA

Key Points:

- Large volumes of precipitation and ground water flow into sanitary-sewer pipes
- This undesirable diversion of water substantially reduces flow in urban streams
- Abatement of this problem could enhance low flows in urban streams by 6%–36%

Supporting Information:

Supporting Information may be found in the online version of this article.

Correspondence to:

L. A. Pangle,
lpangle@gsu.edu

Citation:

Pangle, L. A., Diem, J. E., Milligan, R., Adams, E., & Murray, A. (2022). Contextualizing inflow and infiltration within the streamflow regime of urban watersheds. *Water Resources Research*, *58*, e2021WR030406. https://doi.org/10.1029/2021WR030406

Received 13 MAY 2021
Accepted 19 DEC 2021

Author Contributions:

Conceptualization: Luke A. Pangle, Jeremy E. Diem, Richard Milligan, Ellis Adams
Formal analysis: Luke A. Pangle, Jeremy E. Diem, Allison Murray
Funding acquisition: Luke A. Pangle, Jeremy E. Diem, Richard Milligan, Ellis Adams
Methodology: Luke A. Pangle, Allison Murray
Project Administration: Luke A. Pangle
Visualization: Luke A. Pangle
Writing – original draft: Luke A. Pangle
Writing – review & editing: Jeremy E. Diem, Richard Milligan, Ellis Adams

Abstract Defects in sanitary-sewer infrastructure enable exchange of large volumes of fluids to and from the environment. The intrusion of rainfall and groundwater into sanitary sewers is called inflow and infiltration (I&I). Though long recognized in the assessment of sewers, the impacts of I&I on streamflow within urban watersheds are unknown. We quantified rainfall-derived I&I (RDI&I), groundwater infiltration (GI), and total I&I using measured flows within sanitary-sewer pipes serving four watersheds near Atlanta, Georgia, USA. Flows were monitored in pipes that parallel local stream channels and compared with streamflow measured at nearby gauging sites. Freshwater diverted into the sewer system due to I&I ranged from 24% to 36% of the flow measured within individual pipes. The RDI&I was the smaller component of I&I, ranging from 4.2 to 9.8 mm per year among watersheds. The GI was typically an order of magnitude greater than RDI&I, ranging from 24 to 41 mm per year among watersheds with annual stream discharge of approximately 500 mm. The I&I occurring at specific moments in time commonly represented 0%–20% of the flow measured in the adjacent stream. The enhancement of low flows in streams that could be achievable if I&I were abated ranges from as much as 6%–36% across watersheds. Our discussion presents explanations for the seasonality of I&I and associated impacts on streamflow in urban watersheds, while identifying important sources of remaining uncertainty. Our results support the conclusion that I&I substantially reduces flows in urban streams, especially low flows during dry weather.

Plain Language Summary Water infrastructure degrades over time, allowing for the movement of large volumes of fluids to and from the environment. Inflow is the flow of precipitation into sanitary-sewer pipes through, for example, leaky manholes and gutter downspouts. Infiltration is the flow of groundwater into the same pipes through fractures, leaky joints, and other defects. They cause overflows of untreated sewage that endanger humans and ecosystems. Inflow and infiltration also represent large diversions of fresh water away from local streams. We examined rates of flow in four sanitary-sewer pipes and quantified the inflow and infiltration. We compared these estimates to the rates of flow in nearby streams. We find that inflow and infiltration of fresh water into sanitary-sewer pipes commonly represent 20%–40% of the flow in the pipes. Most of that water emanates from aquifers with a smaller fraction supplied by precipitation. If the inflow and infiltration were abated, and that fresh water instead flowed to stream channels, then the flows in those channels during dry periods could be enhanced by as much as 6%–36%. This is important in urban watersheds, where streamflow during dry weather is already diminished. Inflow and infiltration represent infrastructure-mediated flow pathways that substantially alter the water cycle in urban watersheds.

1. Introduction

Degradation of wastewater infrastructure impacts urban-watershed dynamics in the United States. Defects in sanitary-sewer pipes result in losses of untreated wastewater into the environment. The same defects, in combination with other flow pathways, enable large volumes of precipitation and groundwater to flow into sanitary-sewer pipes (e.g., Pawlowski et al., 2014). The rapid inflow of precipitation and persistent infiltration of groundwater into sanitary-sewer pipes are known as inflow and infiltration (I&I), respectively. Inflow and infiltration are two mechanisms by which water flows between human infrastructure and the landscape may significantly alter the hydrologic cycle within urban watersheds (e.g., Bonneau et al., 2017; Kaushal & Belt, 2012; Mitchell et al., 2003; Vazquez-Sune et al., 2005), although I&I has been less intensively studied than surface runoff (e.g., as reviewed by Walsh et al., 2012; Walsh et al., 2005), and their impact on urban streamflow is poorly understood.

Inflow of water into sanitary-sewer pipes occurs during storms and may persist for many hours after the cessation of precipitation. In this context, infiltration implies a different process than is traditionally defined in scientific hydrology; it represents the temporally variable flow of subterranean water into sanitary-sewer pipes. Flow of groundwater from surrounding porous media into the pipe through a defect should occur only when the pore-water pressure exceeds either the pressure of air within the pipe or the pressure of wastewater anywhere along the submerged interior area of the pipe. These conditions are expected when the water-table surface of an unconfined aquifer rises to, or above, the depth of the pipe (Dirckx et al., 2016). Like inflow, infiltration of groundwater occurs during and shortly following precipitation events, although infiltration may persist over much longer time scales than inflow due to the relatively slow recession of the water table after precipitation has ceased (e.g., Kracht et al., 2007; Kracht & Gujer, 2005; Wittenberg & Aksoy, 2010).

Quantifying I&I during individual storms, and across seasons and years, is commonly done through empirical analysis of a hydrograph measured in either a sewer pipe or at an inflow point to a wastewater treatment plant (WWTP) (e.g., EPA, 2014; Mitchell et al., 2007). Other methods that enable future predictions, but also rely on a measured hydrograph for calibration, include the unit hydrograph approach, the representation of I&I as parallel linear reservoirs (e.g., Deen et al., 1992; Mein & Apostolidis, 1992), and auto-regressive time-series models (Zhang, 2005). In some cases, in situ sensors measure one or more aspects of wastewater chemistry, enabling estimates of I&I based on end-member-mixing analyses (e.g., Bares et al., 2009, 2012; Dirckx et al., 2009; Kracht et al., 2007; Kracht & Gujer, 2005; Zhang, Liu, Cheng, et al., 2018; Zhang, Liu, Dong, et al., 2018; Zhang, 2007). There are also spatially distributed flow and transport models that implement various equations related to the fluid mechanics of pipe networks (Bach et al., 2014; Rauch et al., 2002), which may be used to infer I&I indirectly.

Regardless of the method chosen, the percentage of total wastewater flow that can be attributed to I&I appears to be consistently large. Bares et al. (2009) estimated that I&I may constitute 45% of dry-weather flow in a sanitary sewer in Prague, Czech Republic. Across two sewersheds in Switzerland, I&I ranged from 30 to more than 50% of total wastewater flow (Kracht et al., 2007; Kracht & Gujer, 2005). Dirckx et al. (2009) estimated that I&I constituted at least 50% of dry weather flow in 108 out of 194 watersheds examined in northern Belgium, while also demonstrating the significant spatial variability in I&I that exists longitudinally within pipe networks. Karpf and Krebs (2011) suggest that I&I could be as much as 85% of sanitary-sewer flow in a watershed in Dresden, Germany, while also showing a nearly 10-fold difference in I&I that occurred among pipes of different age and quality.

Inflow and infiltration are threats to the health of humans and aquatic ecosystems and their magnitudes may significantly alter hydrologic cycles within urban and suburban watersheds. In many cases, I&I is the dominant cause of sanitary-sewer overflows (SSOs) (EPA, 2004), which expose humans and terrestrial and aquatic ecosystems to untreated sewage. These SSOs most commonly occur during and shortly after intense storm events when rates of I&I are maximal. Inflow and infiltration represent potentially large diversions of water that may have contributed to evapotranspiration (ET), gross primary productivity, or streamflow generation within low-order stream channels, and an augmentation to flow in the main channel downstream of the WWTP. For example, among multiple storm events, Deen et al. (1992) estimated that 1%–14% of precipitation is routed out of catchments and into sewer systems in Sydney, Australia, while Mein and Apostolidis (1992) approximate typical values around 5% of precipitation. This process could partially subdue peak streamflow during storms in the lower order channels, while also reducing local groundwater storage that supports streamflow and transpiration during drought (e.g., Bhaskar et al., 2015).

Despite the plausible impact of I&I on the hydrologic cycle in urban and suburban watersheds, few studies have contextualized I&I outside the domain of the sanitary-sewer system itself. One salient exception is the study by Bhaskar and Welty (2012), which compared the water balance of urban versus rural watersheds within and around the Baltimore, Maryland metropolitan area. They reported I&I totals from two urban watersheds in the region (sewershed-area-normalized totals of 670 and 460 mm y^{-1}) that were actually greater than the average-annual streamflow among urban watersheds (427 mm y^{-1}). On average, the urban watersheds around Baltimore received approximately 185 mm of additional inflow from irrigation and pipe leakage than did rural watersheds. This represents a significant allotment that could, conceivably, enhance baseflow generation in streams or support transpiration and gross primary productivity of urban ecosystems. However, ET was lesser in urban watersheds—only about 40% of that quantified for rural watersheds—while annual streamflow was only about 15% greater in urban versus rural watersheds. Some fraction of that 185 mm surplus of water inflows, along with a major fraction of annual precipitation (1160 mm y^{-1}), was diverted from these natural flow pathways and unnecessarily

routed into the sanitary-sewer system—predominantly as groundwater infiltration (Bhaskar & Welty, 2012). Wittenberg and Brombach (2002) and Wittenberg and Aksoy (2010) highlight the significance of I&I within the overall hydrologic cycle by reporting, based on some approximate calculations, that conceivably as much as 4% of all river discharge directly into the ocean from Germany is groundwater that was unnecessarily routed through sanitary-sewer networks and WWTPs as I&I.

Aside from these few empirical analyses, the consideration of I&I as a component of the hydrologic cycle in urban watersheds has occurred during the development and implementation of integrated-urban-watershed models (IUWMs) (e.g., see reviews by Bach et al., 2014; Mitchell et al., 2007; Rauch et al., 2002). Many of these models simulate I&I independently and have routing schemes that dictate the interactions between I&I and natural flows (e.g., groundwater recharge and streamflow generation). The foremost objective of these models is to enable predictions of how water management devices (e.g., storm-water-infiltration basins, gray-water conveyance and utilization, etc.) could affect cumulative flows of potable water, wastewater, and meteorically derived flows of water into and out of urban watersheds (e.g., the sequence of works by Mitchell, 2006; Mitchell et al., 2001, 2003, 2008). However, these models are not suitable for highly accurate quantification of I&I. They require specification of myriad numeric parameters, many of which are poorly constrained by available data (as discussed by Mitchell et al., 2007; Rauch et al., 2002). They also require selection of the functional form of equations that are used to simulate receipt, storage, and transmission of water through and between conceptual storages—a selection that may be arbitrary or based on very limited proof of concept. These factors contribute to profound uncertainty in the accuracy of constituent flows and storages within the model, even if cumulative totals of composite flows are reasonably accurate [i.e., the "equifinality" concept discussed by Beven and Freer (2001)].

Our literature review reveals that I&I is common in sewer systems across the United States, Europe, and Australia, while also revealing a lack of fundamental understanding of how I&I alters the hydrology of urban watersheds. It would be wrong to assume that I&I is only relevant to the hydraulics of the pipe system rather than the hydrology of the whole urban watershed. Considering the water balance for a low-order urban watershed, RDI&I and GI represent the mechanisms of water outflow that occur in tandem with stream discharge and evaporation. They contribute to a reduction in surface-water and groundwater storage (Bhaskar et al., 2015)—stores that may otherwise contribute to streamflow, evaporation, or transpiration. But like many other human impacts (Abbott et al., 2019), I&I are commonly overlooked in the conceptualization of the urban hydrologic cycle. The science of watershed hydrology has developed analytical methods that are finding increasing application in urban settings. These include lumped-parameter-transport models for inferring water-residence times within watersheds (e.g., Soulsby et al., 2014), spatially distributed, numerical models of surface and subsurface flows (e.g., Bhaskar et al., 2015; Mittman et al., 2012; Voter & Loheide, 2021), and empirical models that infer relationships between observed streamflow and water storage within the watershed (e.g., Bhaskar & Welty, 2015). As metropolitan governments increase financial investments in water management devices (e.g., green infrastructure and low impact development), these tools and concepts from scientific hydrology have potential applications as change detection tools. Yet, their validity depends explicitly on proper conceptualization of the water-mass balance. Enhancing our understanding of how infrastructure-mediated flows, such as I&I, impact the hydrologic cycle is therefore an imperative area for further inquiry in urban watershed hydrology (Bonneau et al., 2017; Kaushal & Belt, 2012).

Few studies have compared magnitudes of I&I to magnitudes of other stocks and flows in the hydrologic cycle (Bhaskar et al., 2015; Bhaskar & Welty, 2012). The lone study we reviewed that quantified I&I's impact on streamflow did so at the annual time scale (Bhaskar & Welty, 2012). As such, very little is known about the temporal dynamics of I&I's impact on streamflow at intra-annual time scales. Data resources are available to investigate these flow processes, as a growing number of municipalities in the U.S. are investing in monitoring networks that enable more intensive examination of the spatial and temporal dynamics of I&I. To address these research imperatives, we leverage one such monitoring network that spans multiple tributary basins of an urban watershed within the Atlanta, GA region. The objectives of this work are to (1) quantify the temporal dynamics of I&I from daily to seasonal time scales and (2) contextualize the influence of I&I on the overall streamflow regime of low-order watersheds.

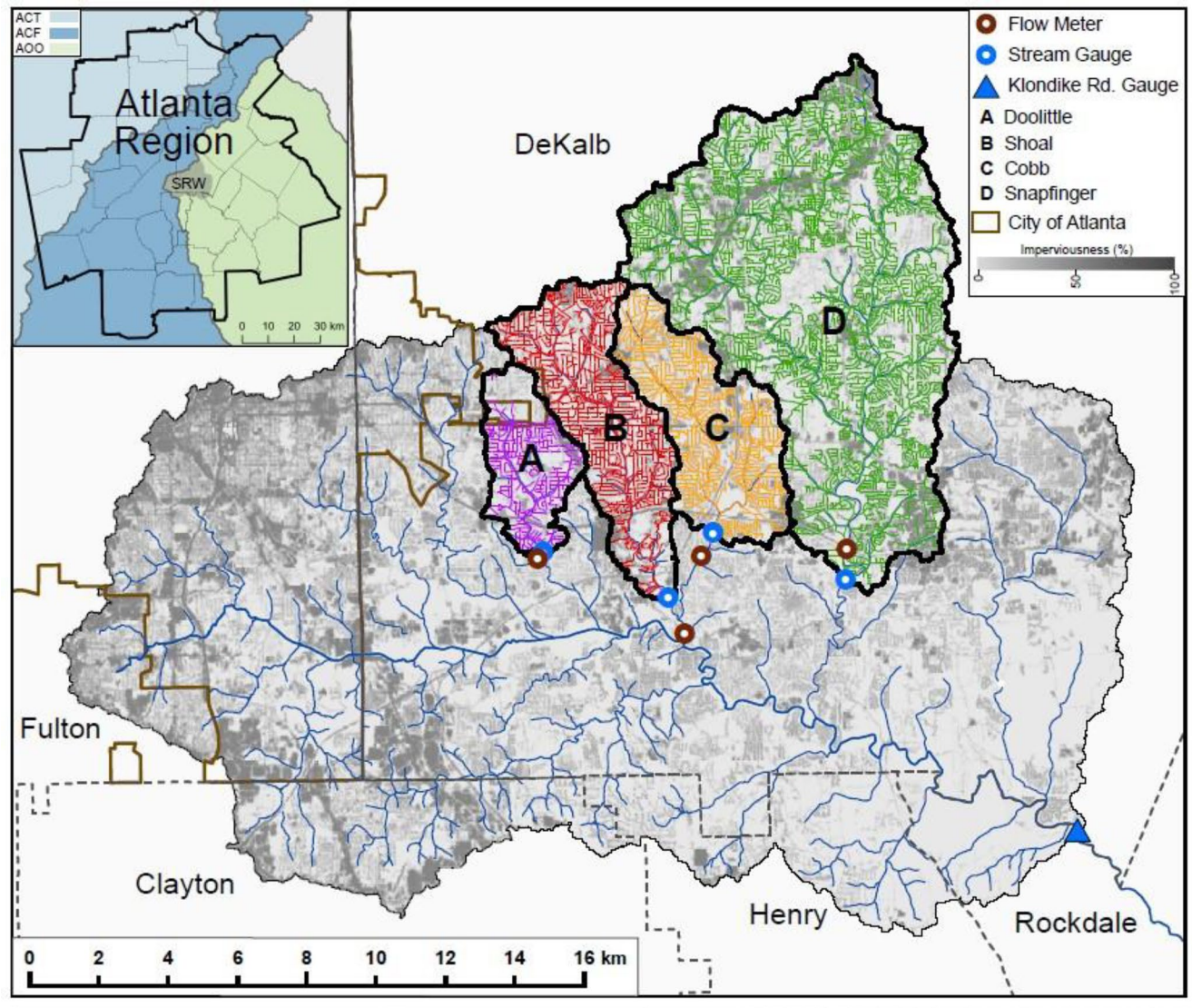

Figure 1. Location of the study watersheds (a–d) within the South River Watershed (SRW), which is in the center of the 30-county Atlanta region. Gravity-drained sanitary sewer pipes (colored lines) are shown for the entire SRW within DeKalb County and within each study watershed. The SRW exists in the Altamaha-Oconee-Ocmulgee Basin, which drains to the Atlantic Ocean, and the two other basins in the Atlanta region are the Alabama-Coosa Tallapoosa Basin and Apalachicola-Chattahoochee-Flint Basin, both of which drain to the Gulf of Mexico.

2. Study Area, Data, and Methods

2.1. Study Area

The study area includes four tributary watersheds within the broader South River Watershed (SRW), located in the Atlanta–Sandy Springs–Gainesville combined statistical area (Figure 1). This 30-county region is the second largest metropolitan area in the southeastern United States with a population exceeding 6 million persons (U.S. Census Bureau, 2020). As defined here, the SRW is determined by the location of USGS gauge 0204070 (i.e., Klondike Road) on the South River. The SRW, which is part of the Altamaha-Oconee-Ocmulgee Basin, exists predominantly within DeKalb County with smaller fractions of the watershed in Clayton, Fulton, Henry, and Rockdale Counties. The four tributary watersheds examined in this study are located entirely within DeKalb County and have similar topography, land cover, and population densities (Table 1). Land cover data representing conditions during 2019 were obtained from the Multi-Resolution Land Characteristics Consortium. We report population densities for each watershed based on the U.S. Census Bureau's American Community Survey, using

Table 1
Description of Study Watersheds

Watershed	Sanitary-sewer meter ID	USGS gauge ID	Elevation range (m)	Area (km^2)	Stream-drainage density (km^{-1})	Pipe-drainage density (km^{-1})	% Impervious Surface Area	% Forested Area	Population density (persons km^{-2})
Cobbs	CBF3-15-101-S005-30	02203873	238–329	20.54	0.79	8.32	26	15	1,201
Doolittle	DOL4-15-107-S045-18	02203831	240–319	10.81	1.01	7.74	22	15	1,264
Lower Snapfinger	LSF4-15-097-S001-48	02203960	230–335	86.18	0.99	7.45	25	19	1,453
Shoal	SHO1-15-070-S010-35	02203863	225–329	22.54	1.26	8.95	24	16	1,334

Note. Watershed name corresponds to the name of the highest order channel draining the watershed. The meter ID is the alphanumeric identifier assigned to specific flow meters within sanitary-sewer pipes. Stream-drainage density is calculated as the total length of perennial stream channels divided by watershed area, while pipe-drainage density is calculated using the total length of sanitary-sewer pipes. For brevity, the actual lengths are not shown, but can be calculated as the product of the relevant drainage density and watershed area.

5-year estimates from the period of 2015–2019. On average, the watersheds are 82% developed with 24% coverage by impervious surfaces and 16% by forested land. Population densities range from 1,201 to 1,453 persons km^{-2}.

The watersheds lie within the Piedmont physiographic province. The terrain is hilly with elevations ranging from 225 to 335 m above sea level. The underlying geology is dominated by crystalline-metamorphic rocks, especially variants of gneiss and schist, with some localized granitic intrusions. Ultisols are the most common soil order in the Piedmont, though soils throughout the area are often categorized simply as urban soil. Soil depth ranges from less than one meter on hillslopes and interfluves to several meters in valley bottoms. Weathered saprolite is pervasive. Total regolith thickness is commonly greater than 10 m with much greater thicknesses reported for low-lying areas. Watersheds are considered geologically isolated from one another with no significant cross-divide movement of groundwater (Cressler et al., 1983; LeGrand, 1967).

The study area has a humid-sub-tropical climate, which is characterized by hot, humid summers and no seasonal differences in precipitation (Trewartha & Horn, 1980). Annual precipitation is approximately 1,300 mm with negligible snowfall (Konrad & Fuhrmann, 2013). Potential ET within forested, tributary watersheds of the South River reaches maximal values from late June through August. Due to increasing ET and episodic precipitation events, soil water and groundwater storage experience net declines usually beginning in April. Cumulative potential ET may exceed cumulative precipitation during summer and early autumn, leading to seasonally water-limited conditions (e.g., Aulenbach & Peters, 2018; Peters & Aulenbach, 2011).

2.2. Data Resources

The analysis uses time-series measurements of precipitation and pipe-flow rates obtained through open-records request, and that are collected as part of the DeKalb County Department of Watershed Management's Capacity, Management, Operations, and Maintenance Program (DWM, 2015). That network includes approximately 200 monitoring locations within DeKalb County. Out of the approximately 100 flow meters that existed within the SRW, we selected four that were installed on main trunk lines and that were closest to existing USGS stream gauging sites (Table 1). We obtained data for calendar year 2019. Flow rates within sanitary-sewer pipes were monitored with acoustic-doppler sensors that yield measurements of depth [L], velocity [$L\ T^{-1}$], and flow [$L^3\ T^{-1}$]. The sensors were logged at 15-min intervals and the flow was recorded in gallons per minute. Initial review of the data showed infrequent occurrences of zero, or negative, flow values, which were apparently due to episodic sensor malfunction. These values were removed from the data set. The percent of 15-min intervals for which data were omitted from the monitors listed in Table 1 was 5.4%, 0.2%, 3.6%, and 0.2%, respectively. These were scattered across the time series and we did not try to fill the gaps. Tipping bucket rain gauges were collocated (aboveground) with the in-pipe flow meters at two of the four locations. The westernmost rain gauge was applied to Doolittle and Shoal Creek watersheds, while the easternmost gauge was applied to Cobbs Creek and Lower Snapfinger Creek watersheds. Cumulative precipitation estimates from these devices were logged at a 15-min interval and reported in units of inches.

We used time series of streamflow, measured at 15-min intervals, obtained from USGS stream gauging stations located on each tributary watershed. The stream gauges and sanitary-sewer flow meters shown in Table 1 were

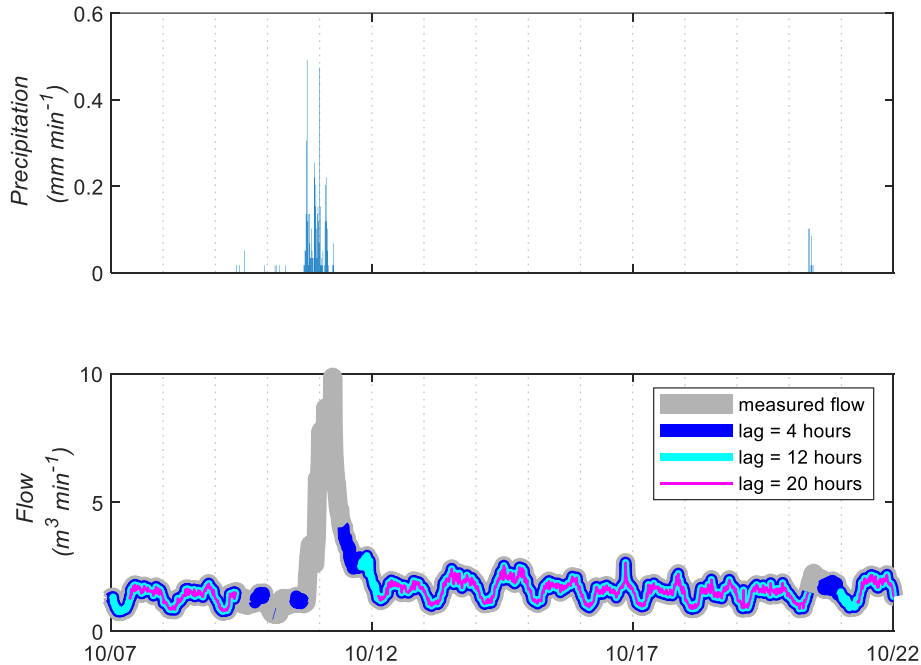

Figure 2. Time series of precipitation (top) and pipe flow (bottom) from 10/7/2018 to 10/22/2018 at the DOL4-15-107-S045-18 monitoring station. Gray line represents measured flow. Each of three colored lines represent the duplicate data set that results after converting flow values to NaN (i.e., "not a number") during, and for variable lag times following, precipitation occurrences. Breaks in the colored lines represent time intervals over which we interpolate the flow that would have occurred in the absence of precipitation, using the moving-window-averaging technique described in the text. Rainfall-derived I&I is calculated as the difference between measured and interpolated flow during those intervals.

separated by linear distances ranging from approximately 222 to 1,160 m (Figure 1). Table 1 summarizes the area, elevation range, and drainage densities for the tributary watersheds draining to each gauging station. Table 1 also shows the pipe-drainage density, which is the total length of gravity-main-sanitary-sewer pipes divided by the same watershed area. Notably, the length of sanitary-sewer pipe within each watershed is greater than the length of perennial stream channels by factors of approximately six to ten. The shapefile showing the gravity-drained sewer pipes in the Doolittle Creek watershed was incomplete with part of the northern extent of the watershed unrepresented (Figure 1). We calculated the pipe-drainage density for the area of the watershed where the shapefile coverage was complete and then extrapolated that density to the whole watershed area. None of these stream gauging locations is influenced by discharge from WWTPs. When measured flows in pipes and stream channels are reported as area-normalized flows in our results, we have divided those volumetric flows by the topographically delineated area of the respective watershed (Table 1).

2.3. Quantifying Rainfall-Derived Inflow and Infiltration

Our approach to quantifying rainfall-derived I&I (RDI&I)—the I&I occurring during and shortly after precipitation events—included three steps. First, we identified intervals within the time series of pipe flow that occurred during precipitation events or for some specified period (hereafter referred to as lag time) after precipitation had ceased. A time series of pipe flow is illustrated in Figure 2, showing multiple days with and without precipitation. On days with no precipitation, the pipe flow follows a cyclical pattern showing minimal values during the night and early morning then greater values during daylight hours. This pattern is explained by the diurnal variation in wastewater generation by people and industry. During and after some precipitation events, there are marked increases in pipe flow that deviate substantially from this pattern. These exceptional flows are reasonably assumed to reflect the inflow of current precipitation and infiltration of existing groundwater into the sewer pipes. We created a duplicate times series of pipe flow that is identical to the original data, except that we replace numeric values with the code "NaN" (indicating "Not a Number") when (1) precipitation accumulation over the previous 15 min was greater than zero, and (2) for a 32-hr lag time following the cessation of precipitation. The lag time

was chosen based on a simple sensitivity test, whereby we calculated cumulative estimates of RDI&I and RDI&I as a percentage of total pipe flow, using lag times of 4–40 hr, at four-hour intervals (Figure S1 in the Supporting Information S1). At relatively short lag times, it was commonly observed that the range of times during which pipe-flow values were converted to NaN did not fully encompass the observed deviations in flow that resulted from RDI&I (Figures 2 and S1 in the Supporting Information S1). This type of exclusion was avoided at a time lag of 32 hr. For precipitation events that caused no apparent RDI&I (e.g., 10/20/2018 from Figure 2), a greater lag time increases the probability that a nonzero magnitude of RDI&I will be calculated, even though the hydrograph shows little evidence of an effect of RDI&I at all. We implemented a second calculation, described later, that helps to nullify this potential problem.

In the second step, we interpolated plausible values of pipe flow during those time increments when the actual measured values were replaced with NaN. Our approach is similar to the approach of Mein and Apostolidis (1992) for separating RDI&I from the persistent pattern of so-called dry-weather flow. The interpolated values are meant to represent the likely flow that would have occurred in the absence of precipitation. We used a simple moving-window-average calculation as shown below:

$$Q_{\text{int},t} = \frac{1}{n}\sum_{i=1}^{i=n} Q[t + \Delta t(i)] \tag{1}$$

where $Q_{\text{int},t}$ is the interpolated flow at time t; Δt is a vector of time increments (hours) with length n, and i indexes the individual values within Δt. The initial values assigned to that vector were −48, −24, 24, and 48. The result represents the average pipe flow measured at the same moment in time on the previous two and following two days. In some cases, the measured pipe flow at those preceding and following times may have also been converted to NaN due to the occurrence of precipitation. In that case, the values within Δt were allowed to decrease or increase by increments of −24 and 24, respectively, up to minimum and maximum values of −240 and 240, respectively. In other words, the moving average may be calculated using measurements that occurred up to 10 days before or after the current time, while maintaining $n = 4$. In some cases, n was less than four, due to extended periods of frequent precipitation.

In the third step, the rate of RDI&I was calculated at each moment in time delineated in step one above as

$$RDI\&I = Q_t - Q_{\text{int},t} \tag{2}$$

where Q_t is the measured pipe flow at time t. Given the 15-min interval of data recording, we assumed this rate was representative of the whole 15-min period preceding the measurement and multiplied by 15 min to obtain the volume of RDI&I over that time increment. These volumes were summed over time to obtain cumulative RDI&I.

An important observation is that not all precipitation events caused deviations in measured pipe flow that exceed the typical range observed during rainless periods. The procedure described in the first step above does not specifically exclude these time periods from the eventual estimation of RDI&I as shown in Equation 2. Instead, we utilized a simple filtering approach to discount values of RDI&I from Equation 2 that are lesser than the approximate error associated with the interpolation scheme. To approximate that error, we used a basic split-sample test. Equation 1 was applied to estimate values of $Q_{\text{int},t}$ at every moment in time for which there was a non-NaN value in the duplicate time series described in step one—that is, at every moment not influenced by RDI&I. The length of this time series varied for each sensor but was on the order of 10^5 data points for all. Scatter plots of Q_t versus $Q_{\text{int},t}$ were developed from these time increments for each sensor and compared to a line with slope of one. In all cases, the residuals appeared symmetrically distributed around that line, implying no systematic error (see Figures S2–S5 in the Supporting Information S1). Using the absolute value of these residuals, we determined the magnitude of the residual constituting the 99th percentile of their distribution, $|R_{99}|$ and applied the following condition:

$$if \quad RDI\&I < |R_{99}| \qquad then \quad RDI\&I = 0 \tag{3}$$

In other words, if the calculated value of RDI&I from Equation 2 is less than the inherent error of the interpolation scheme (Equation 1), then the value is converted to zero.

2.4. Calculating Groundwater Infiltration

The second component of total I&I is groundwater infiltration (GI) that occurs during and between precipitation events and across seasons. Time series of sanitary-sewage flow often show persistently higher values during the winter and spring seasons, which gradually decline throughout the summer toward minimum values that typically occur in late summer or early autumn (e.g., Bares et al., 2009; Diem et al., 2021; Dirckx et al., 2009). This pattern is attributed to enhanced GI occurring during cold seasons when groundwater storage and the water-table elevation are relatively high and relatively lower rates of GI during warm seasons when the water-table elevation has decreased (Figure S6 in the Supporting Information S1). Though varied in detail, most methods for quantifying GI that rely on a measured hydrograph of wastewater flow do so by (1) identifying a time increment where GI is assumed to minimal and (2) calculating putative GI at any time as the difference between pipe flow at that time and the minimal observed rate of GI. We adopt a similar approach that is outlined below.

For each day in our time series, we calculated a 7-day-moving-window average of the measured flow within the sanitary-sewer pipes from 3:00 to 5:00. We did this using the interpolated time series, including estimates of $Q_{\text{int},t}$ from Equation 1, to avoid any influence of RDI&I on the averages. This average represents the combination of some persistent, overnight generation of wastewater and GI, as shown below:

$$\overline{Q}_{\text{pd}} = \overline{\text{SS}}_{\text{pd}} + \overline{\text{GI}}_{\text{pd}} \tag{4}$$

where $\overline{Q}_{\text{pd}}$ is the average-measured flow during the pre-dawn hours of 3:00–5:00, while $\overline{\text{SS}}_{\text{pd}}$ and $\overline{\text{GI}}_{\text{pd}}$ are the average sanitary-sewage flow and GI into the pipes over the same time interval, respectively. We chose 3:00–5:00 as the time increment for averaging based on the assumption that $\overline{\text{SS}}_{\text{pd}}$ would be most consistent across days and seasons during this time interval. In other words, the sources of wastewater generation during these pre-dawn hours—for example, wastewater from overnight shift workers and 24-hr businesses, overnight operation of washing machines in restaurants, flushing of heating/cooling system components, discharge from automated manufacturing processes, etc.—are assumed to be generating wastewater volumes consistently throughout the year.

Among all days in 2019, we identified the minimum value of $\overline{Q}_{\text{pd}}$ for each monitored pipe location ($\overline{Q}_{\text{pd,min}}$). For each day, we then we calculate the difference:

$$\text{GI}_d = \overline{Q}_{\text{pd},d} - \overline{Q}_{\text{pd,min}} = \overline{\text{SS}}_{\text{pd},d} + \overline{\text{GI}}_{\text{pd},d} - \overline{\text{SS}}_{\text{pd,min}} - \overline{\text{GI}}_{\text{pd,min}} \tag{5}$$

where *"d"* and "*min*" are added to the subscripts to indicate the average values calculated on a specific day from 3:00 to 5:00 and the minimum value of each average, respectively. GI_d is the estimated rate of groundwater infiltration occurring from 3:00 to 5:00 on a particular day, which is further assumed to be a representative rate for the entire 24-hr day. We have assumed that the rate $\overline{\text{SS}}_{\text{pd}}$ will be relatively stable across days and seasons, which leads to the approximation $\overline{\text{SS}}_{\text{pd},d} \sim \overline{\text{SS}}_{\text{pd,min}}$. Given that assumption, Equation 5 is rewritten as below.

$$\text{GI}_d = \overline{Q}_{\text{pd},d} - \overline{Q}_{\text{pd,min}} = \overline{\text{GI}}_{\text{pd},d} - \overline{\text{GI}}_{\text{pd,min}} \tag{6}$$

If $\overline{\text{GI}}_{\text{pd,min}} = 0$, then GI_d is a reasonable estimate of the absolute rate of groundwater infiltration occurring on a particular day, at least under the assumptions we have outlined. If $\overline{\text{GI}}_{\text{pd,min}} > 0$, then GI_d is only an estimate of the difference in groundwater infiltration occurring during the current day, and the day when *GI* is minimal. It is also conceivable that $\overline{\text{GI}}_{\text{pd,min}} < 0$, implying that exfiltration from the pipes into the aquifer is greater than GI over the entire pipe network draining to a measurement point. Prior studies suggest that exfiltration rates are inhibited due to clogging of defects by sediment and other solids in the wastewater flow (e.g., Blackwood et al., 2005; Ellis et al., 2003) and may be one to more orders of magnitude lower than freshwater infiltration rates (e.g., Karpf et al., 2011). Further, it is very likely that at least some portions of the pipes remain inundated by groundwater throughout the year in these watersheds (Figure S6 in the Supporting Information S1). Based on those two lines of evidence, we discount the possibility that net exfiltration over the pipe network ever exceeds net infiltration. Lacking an extensive network of wells to monitor actual water-table elevation and complete knowledge about the spatial distribution of pipe defects that would allow GI to occur, we proceed with the assumption that $\overline{\text{GI}}_{\text{pd,min}} = 0$. This and the alternative assumptions noted above are discussed more thoroughly in Section 4.4. This assumption implies that inter-watershed comparisons of GI_d and total *I&I* must be interpreted cautiously. The outcome of such a comparison could prove to be qualitatively different if the magnitude of $\overline{\text{GI}}_{\text{pd,min}}$ were truly known. However, even if $\overline{\text{GI}}_{\text{pd,min}} > 0$, that rate is likely relatively low and a small fraction of total GI. We present some

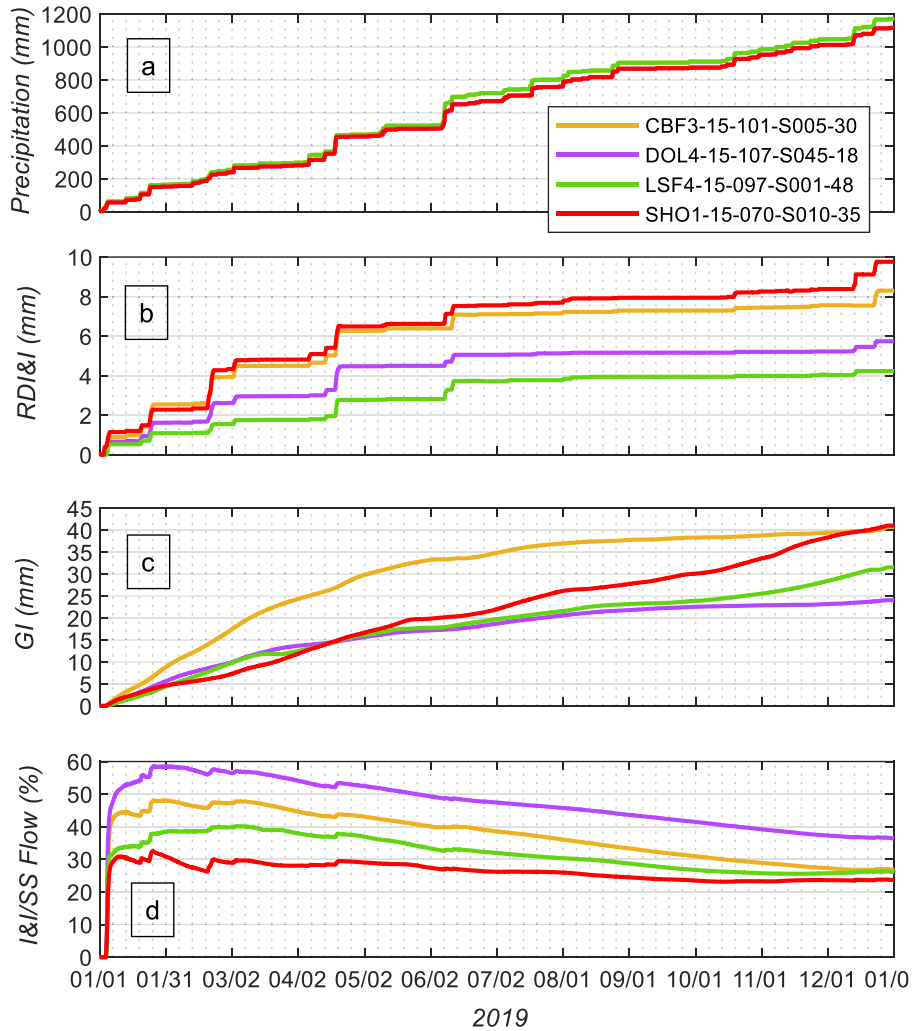

Figure 3. Time series of (a) cumulative precipitation, (b) cumulative rainfall-derived I&I, (c) cumulative groundwater infiltration, and (d) total I&I (RDI&I + GI) divided by total sanitary-sewage flow. All cumulative flows are divided by the respective watershed area and reported as area-normalized depth (mm). Legend entries correspond to the monitor identification codes shown in Table 1. Line colors correspond with colors used to represent pipe networks for each watershed within Figure 1.

inter-watershed comparisons in the latter part of our results under the assumption that they are qualitatively correct, even though those comparisons could deviate somewhat numerically if $\overline{GI}_{pd,min} > 0$.

3. Results

The 2019 calendar year was drier than average. Total precipitation measured across monitoring locations ranged from 1,116 to 1,171 mm with an average of 1,143 mm (Figure 3a). This is 130 mm less than the average-annual precipitation for eight basins in the Atlanta Metropolitan region reported by Diem et al. (2018), and 105 mm less than the average reported for the nearby Panola Mountain Research Watershed (Aulenbach & Peters, 2018)—both studies leveraging data sets spanning approximately 30 years. The low precipitation total is partially attributable to a severe drought that was onset in late August and persisted into early October (Figure S7 in the Supporting Information S1).

Both RDI&I and GI varied widely among the four watersheds, though GI was consistently greater than RDI&I in all watersheds. The cumulative RDI&I calculated during 2019 ranged from 4.2 mm in Lower Snapfinger Creek watershed to 9.8 mm within the Shoal Creek watershed (Figure 3b). The cumulative GI calculated during 2019

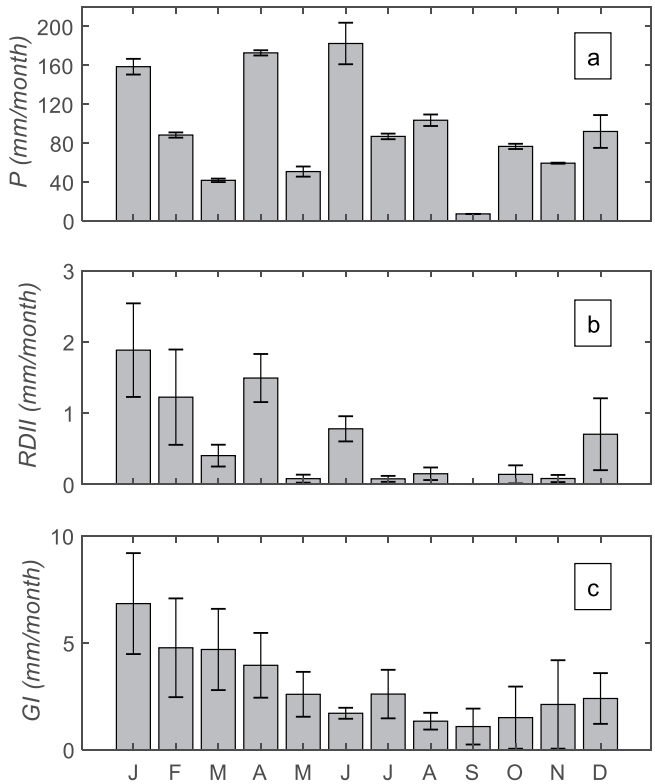

Figure 4. Variations in (a) total-monthly precipitation, (b) rainfall-derived infiltration and inflow, and (c) groundwater infiltration averaged among all monitoring locations. Error bars indicate the standard deviation among measurement locations.

ranged from 24.1 mm within Doolittle Creek watershed to 41.1 mm within the Shoal Creek watershed (Figure 3c). The cumulative GI was greater than cumulative RDI&I by factors ranging from 4.2 to 7.5 across watersheds. Watersheds where RDI&I was relatively large also tended to have relatively large totals of GI. Though there are only four data points, the correlation between cumulative RDI&I and GI (expressed as area-normalized depths) has a coefficient of determination of 0.62, suggesting some similarity in the flow pathways by which RDII and GI enter the sanitary-sewer pipes.

Inflow and infiltration had the greatest impact on total flow within sanitary-sewer pipes in winter. From January through March, cumulative I&I regularly constituted 25%–55% of the cumulative flow measured within the pipes. The percentage declined throughout the remainder of the year, yet even during late summer and fall I&I commonly comprised 20%–40% of the total measured flow across pipes. There was no clear correspondence between the magnitude of I&I (the sum of RDI&I and GI in Figures 3b and 3c) and I&I expressed as a percent of total pipe flow. For example, area-normalized depths of RDI&I and GI were greatest within the Shoal Creek watershed (Figures 3b and 3c), although the magnitude of I&I relative to total measured flow in the pipe was lowest for Shoal Creek (Figure 3d). Hence, a relatively low rate of I&I observed within the sewer system may actually correspond to a relatively large area-normalized flow of water within the basin's water budget.

The variability in rates of RDI&I and GI across months and seasons is similar to the temporal variability of streamflow generation. Precipitation is distributed across all months, notwithstanding the considerable month-to-month variability and the pronounced drought period that spanned from late August through early October (Figures 4a and S7 in the Supporting Information S1). The average-monthly RDI&I was correlated with average-monthly precipitation across the year (R^2 = 0.53). The correlation was stronger when the monthly averages (Figure 4) were grouped from January through May (RDI&I = 0.0112 × P – 0.1346; R^2 = 0.82) and June through November (RDI&I = 0.0045 × P – 0.1795; R^2 = 0.81), the main difference between those periods being the approximately 2.5-fold greater slope for the former period. The monthly totals of GI show less sensitivity to the monthly differences in total precipitation. Correlations between average-monthly precipitation and GI (Figure 4) show R^2 values of 0.11, 0.22, and 0.05 for the entire year and the two groupings of months noted above, respectively. For example, the large precipitation total in April generated the second largest average-total RDI&I across monitoring locations—a total that was markedly higher than the previous, and drier, month of March. However, the average-total GI in April was nearly identical to the amount observed in the drier month of March (Figure 4c). Groundwater infiltration continued to occur in September, even though average-total RDI&I among monitoring locations declined to only 22 m^3 (a negligible area-normalized depth). There was large variability among sites in both RDI&I and GI during any given month. The coefficient of variation was always greater than 0.5 and commonly exceeded one for both variables.

The impact of I&I on streamflow is dynamic in response to storm events. The time series of I&I as a percentage of streamflow for Shoal Creek shows abrupt increases that in some cases exceeds 100% (Figure 5). These are transient, often occurring over a single 15-min measurement interval, and in most cases appear to occur just before the associated rise in the stream hydrograph. These abrupt rises may be partly explained by the rapid intrusion of precipitation into sanitary-sewer pipes through leaky manholes, connected downspouts from gutters, or other mechanisms that deliver new precipitation into the pipe network moments before it even reaches the stream. These transient spikes with magnitude of 100% or greater were not observed in the other three watersheds (Figures S8–S10 in the Supporting Information S1). For Shoal Creek (Figure 5) and Lower Snapfinger Creek (Figure S10 in the Supporting Information S1), the I&I as a percentage of streamflow is minimal during the winter and spring and then becomes maximal during the late summer and early fall seasons when total streamflow is near seasonal minimum values. For Cobbs Creek (Figure S8 in the Supporting Information S1), nearly the opposite

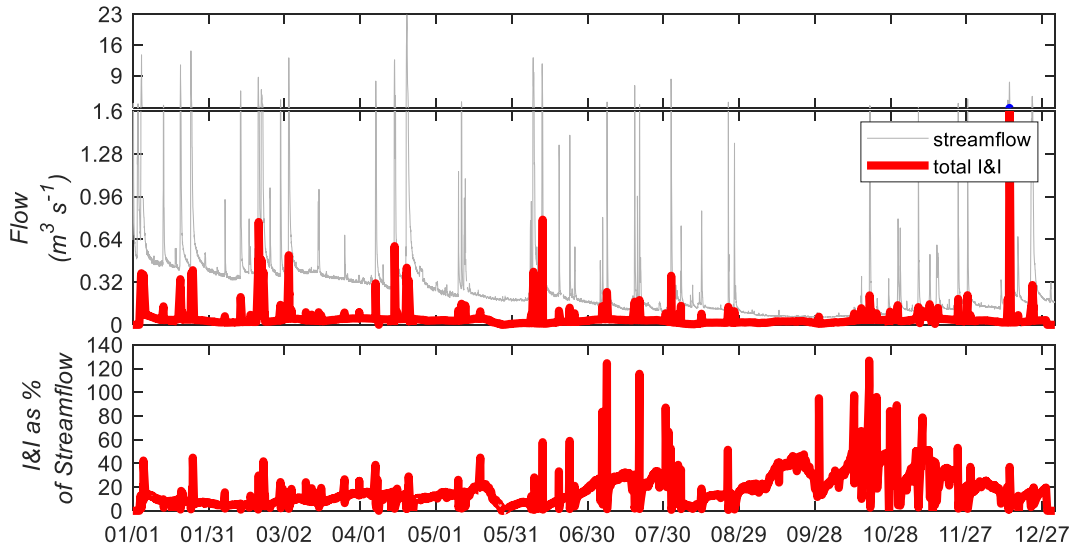

Figure 5. The top graph shows time series of streamflow at USGS Gauge 02203863 (Shoal Creek) and the calculated time series of total I&I – the sum of rainfall-derived I&I and groundwater infiltration. Note the presence of an axis break on the vertical axis, which enables better visualization of both time series across their full range. The bottom graph shows a time series of total I&I as a percentage of streamflow. Line color corresponds to the color used to represent the pipe network for this watershed in Figure 1.

pattern was observed, and for Doolittle Creek, there was not pronounced seasonality in I&I as a percentage of streamflow (Figure S9 in the Supporting Information S1).

The impact of I&I on streamflow was dynamic in response to daily- and seasonal-hydroclimatic variability, and variable among the watersheds we studied (Figure 6). Frequency distributions show I&I expressed as a percentage of streamflow for all watersheds, where frequencies are calculated for 2% intervals of the variable *I&I*/streamflow × 100. In some cases, this percentage is narrowly distributed, suggesting some similarity in the temporal dynamics of streamflow-generating and I&I-generating flow processes. For example, in the Doolittle Creek watershed, I&I as a percentage of streamflow is almost always between zero and 20% with pronounced peak frequencies occurring at 4%–8% (Figure 6b). Within the other three watersheds, I&I as a percentage of streamflow reaches, or exceeds, 30% with the greatest frequencies occurring in the range of 4%–18%. A broader range of I&I impacts on streamflow (Figures 6a, 6c, and 6d) implies less similarity (or proportionality) in the temporal dynamics of streamflow- and I&I-generating flow processes. Especially for Lower Snapfinger and Shoal Creek watersheds, the frequency distributions have pronounced positive skew, suggesting that those conditions that facilitate especially strong impacts of I&I on streamflow are relatively short in duration (Figures 6c and 6d).

The impact of I&I and streamflow and the contrasts among the urban watersheds in this study are further illustrated through flow-exceedance-frequency analysis (Figure 7). The horizontal axis shows cumulative frequency of exceedance; the vertical axis shows the instantaneous measurement of streamflow associated with that cumulative frequency (a.k.a., flow-duration curves). The solid lines are based on the measured streamflow. The dashed lines represent the sum of measured streamflow and calculated I&I at every 15-min measurement interval, thus indicating the positive effect on streamflow rates that would occur if all the I&I were instead discharged into the local stream channel. The streamflow magnitudes associated with exceedance frequency of 0.75 were relatively consistent across the four watersheds, ranging between 5 and 6×10^{-6} mm s^{-1}. In some cases, the impact of I&I on streamflow (as depicted by the dashed lines) was relatively consistent across the range of exceedance frequencies 0.75–0.99 (e.g., Figures 7b and 7c), whereas in other cases, the impact somewhat diminished when streamflow was near its minimal observed value (Figures 7a and 7d). Considering a broader range of exceedance frequencies, there was a prevailing pattern of I&I more strongly influencing mid-range and low-flow magnitudes (Figure 8). The more pronounced impact on streamflow magnitudes associated with the 0.75–0.99 frequencies of exceedance was apparent for Lower Snapfinger and Shoal Creek watersheds and evident but more subtle for Doolittle watershed. In contrast, Cobbs Creek watershed was the only case where high-flow magnitudes were more strongly impacted by I&I than were low-flow magnitudes. Specific low flows (75th–99th cumulative-exceedance

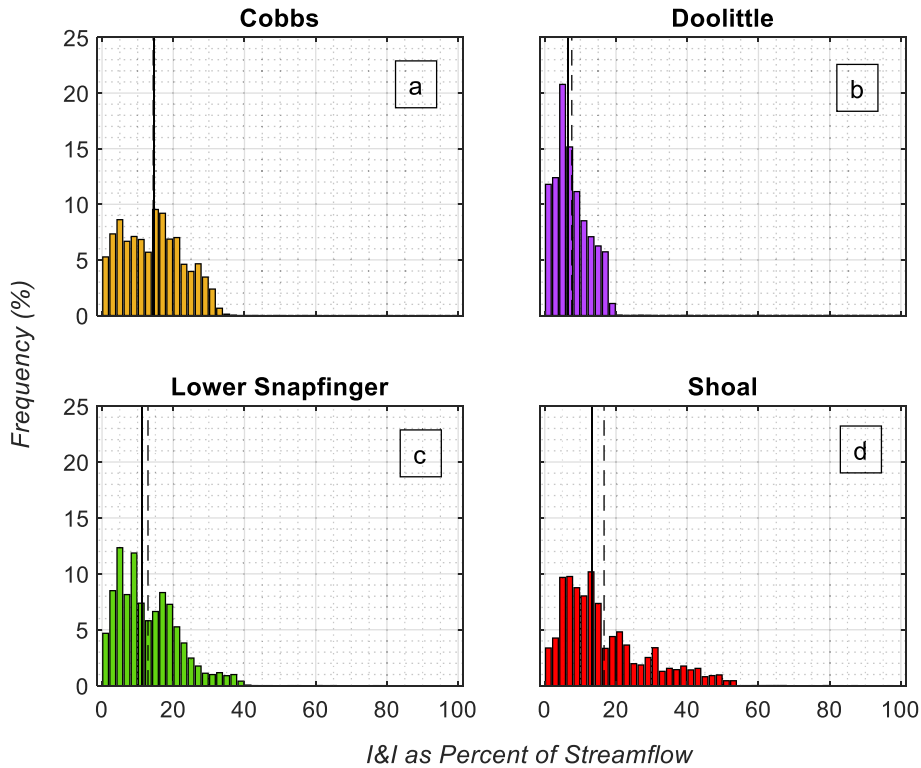

Figure 6. Frequency distributions of I&I expressed as a percentage of streamflow measured in the nearby channel. Both variables are quantified at 15-min intervals. The vertical axis represents the percent of all measurements taken in 2019 at that time interval. Bar colors correspond to the colors used to represent pipe networks in each watershed in Figure 1. The solid and dashed black lines indicate the median and mean of the distributions, respectively.

frequencies) could possibly increase by 6%–36% across the tributary watersheds examined here. High flows (1st–25th cumulative-exceedance frequencies), often associated with urban flooding, would conceivably be enhanced by 1%–27%.

4. Discussion

4.1. Cross-Study Comparison of I&I Effects on Urban Streamflow

Similar to the findings of other studies, our results demonstrate that I&I constitutes a substantial amount of the total flow within sanitary-sewer pipes in urban and suburban watersheds. Among four watersheds, and spanning calendar year 2019, we observed that I&I commonly constituted 20%–40% of the pipe flow and exceeded 40% during the cold season for two watersheds (Figure 3). These results are comparable, or slightly lesser, than the I&I as a percentage of total pipe flow reported from multiple study systems across Europe (Bares et al., 2009, 2012; Dirckx et al., 2009; Kracht et al., 2007; Kracht & Gujer, 2005), and notably lower than reports from other European (Karpf & Krebs, 2011) and American cities (Bhaskar & Welty, 2012). These estimates are generally higher than those reported by Cahoon and Hanke (2017) for systems within the coastal plain province of North Carolina, USA. Our results agree with those previous studies that have demonstrated that GI is a considerably larger component of I&I than is RDI&I (e.g., Karpf & Krebs, 2011; Kracht & Gujer, 2005; Wittenberg & Aksoy, 2010). This outcome will clearly depend on how frequently the pipes are inundated by groundwater and over what spatial extent. Through model simulations of groundwater levels and pipe-flow dynamics, Karpf and Krebs (2011) show that the duration of inundation by groundwater for specific pipe sections ranged from 26 to 361 days in Dresden, Germany. Such durations are not possible to infer in the absence of accurate, basin-wide measurements or simulations of water-table position. Nonetheless, in humid watersheds with low relief and water-table depths that are consistently near pipe installations, it is perhaps reasonable to assume that persistent GI will be greater than the more episodic RDI&I. Despite contrasting landscapes, age and type of infrastructure, population density, and

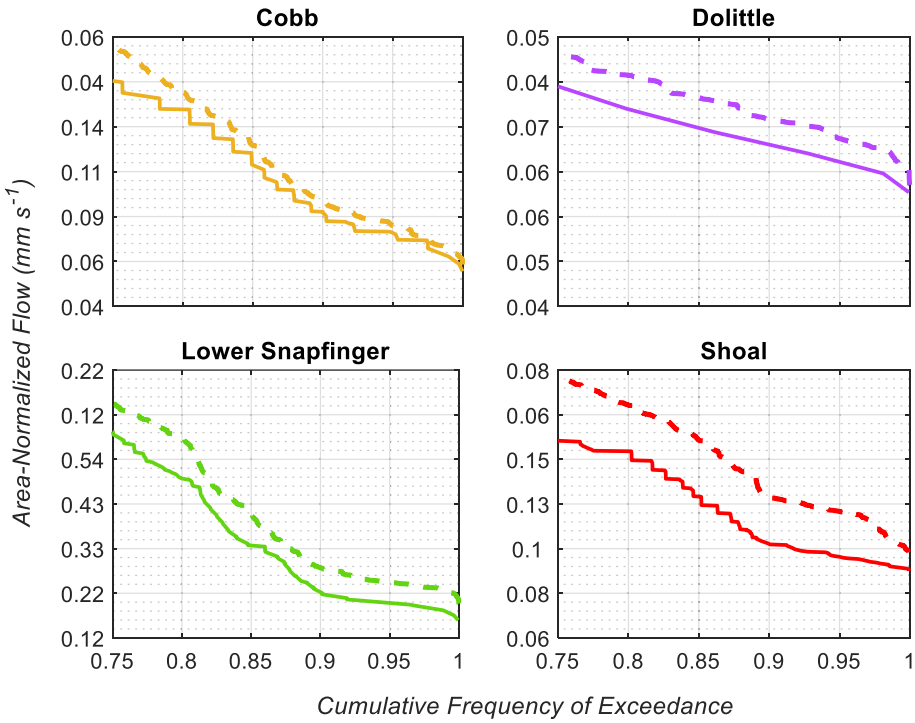

Figure 7. The relationship between the cumulative frequency of exceedance and instantaneous measures of streamflow (a.k.a., flow-duration curves; solid lines) at USGS stream gauging stations within the four studied watersheds. The dashed lines show the increase in flow associated with each frequency of exceedance that would occur if all I&I entering sanitary-sewer pipes were instead discharged into the stream channel. The horizontal axis is constricted to frequencies of exceedance ranging from 0.75 to 1 to enable better visualization of the potential impact of I&I on the associated lower quartile of streamflow magnitudes.

method of calculation, the results from these studies and our own support the notion that I&I is ubiquitous and consistently a high fraction of the total flow in sanitary-sewer systems in humid-temperate climates.

The comparison of our results with those presented by Bhaskar and Welty (2012) reveals a remarkable contrast in the relative impacts of I&I on streamflow regimes in urban watersheds. Bhaskar and Welty (2012) reported average I&I across two watersheds in Baltimore, MD USA as 565 mm/y, which was approximately 22% greater than streamflow (465 mm) and 57% greater than evapotranspiration (360 mm) from those two watersheds over the same time increment. Hence, as an area-normalized depth of water, I&I was the single largest flux of water out of each watershed. Our estimates of I&I as an area-normalized flow are an order of magnitude lower (30–51 mm; Figure 3). Our results across four watersheds showed that I&I represented a significant, though typically minority, fraction of the volume of streamflow. Expressed as a percentage of streamflow, I&I was most often in the range of 0%–20%, though it approached or exceeded 40% in some cases (Figure 6). The differences between our results and those of Bhaskar and Welty (2012) may be attributable to a more severely degraded sanitary-sewer system in the Baltimore-versus Atlanta-Metropolitan area. They cite several government reports, suggesting that I&I constituted 50%–90% of total flow in sanitary-sewer pipes monitored across multiple sewersheds. That is a generally higher percentage than we found, though similar in order of magnitude. Differences may also arise due to study organization and data normalization. We were able to leverage a network of in-pipe meters that included units installed closely to USGS stream gauging locations. We compare I&I within sanitary-sewer trunklines delivered by a pipe network that exists mostly (though not entirely; Figure 1) within the topographic boundaries of the watershed that drains to the nearby stream gauging station. Bhaskar and Welty (2012) note in their discussion that due to limits on available data sources, the overall contributing areas to stream channels and sanitary-sewer pipes were not the same. Thus, their comparison of area-normalized fluxes is perhaps not an equal comparison if the respective volumetric flows are normalized by different contributing areas. Nonetheless, both studies emphasize that I&I is a significant perturbation to streamflow regimes in urban watersheds, especially to the low-flow regime during dry weather conditions.

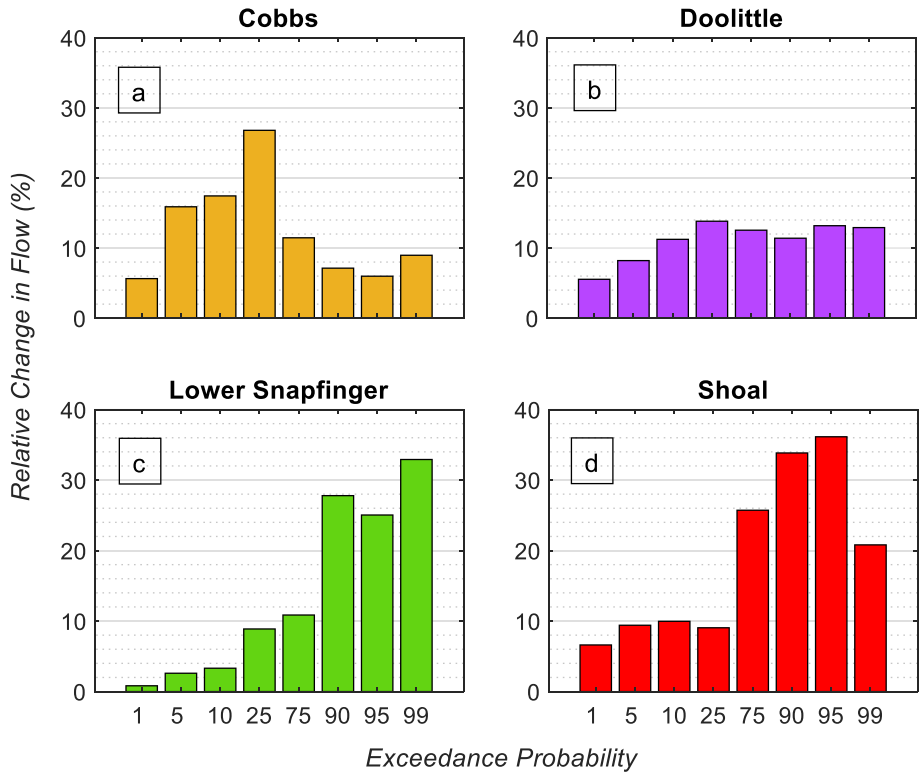

Figure 8. The vertical axis shows the potential, relative increase in streamflow magnitude that would be possible if no I&I occurred, and all associated water was instead discharged into local stream channels. The horizontal axis values correspond to selected probabilities from the cumulative probability distributions of flow exceedance (e.g., as shown in Figure 7).

4.2. Hydrologic Drivers and Seasonality of I&I Mirror Those of Natural Streamflow

To our knowledge, this is the first study to demonstrate how streamflow is modulated by I&I at intra-annual time scales. Our results reveal marked correspondence in the temporal dynamics of I&I and streamflow generation from daily to monthly time scales, suggesting some similarity in the underlying hydrologic mechanisms. Similarities include [compare Figures 4 and 5 to the results from (Aulenbach & Peters, 2018)] greater rates and responsiveness to precipitation events during winter and spring than in summer and fall; greater contributions from groundwater flow than from surface- or soil-water flow; enhanced groundwater flow during cold, water-surplus seasons and vice versa, driven by seasonal fluctuations in water-table depths and prevailing hydraulic gradients within local unconfined aquifers. Our interpretation of the mechanisms underlying these observations is described below.

We reason that the seasonality of RDI&I is controlled by seasonal variation in the soil-water content and evapotranspiration, similar to the effects those processes exert on seasonal streamflow. The rapid delivery of RDI&I into sanitary-sewer pipes occurs via leaky manhole casings, inappropriately routed gutter downspouts, and through leaky or fractured pipes and joints (Pawlowski et al., 2014). More generally, though, these flow pathways may be conceptualized as "fast" mechanisms of water delivery to sanitary-sewer pipes that are analogous to mechanisms of rapid streamflow generation in Piedmont watersheds. Some examples of the latter include infiltration-excess overland flow, saturation-excess overland flow, and lateral flow of groundwater that accumulates in transient, perched aquifers within surficial soil horizons (e.g., Burns, 2002; Freer et al., 2002; Zimmer & McGlynn, 2017). The latter two mechanisms become less prevalent during summer and fall due to soil dehydration—evapotranspiration in excess of precipitation increases vacant porosity within soils and reduces the likelihood of water saturation and positive pore-water pressure head (Aulenbach & Peters, 2018). Similarly, positive pore-water pressure would be required for subterranean water to flow across soil-pipe or soil-manhole interfaces, though this condition would be less likely to occur during any storm event when soils are relatively dry (Dirckx et al., 2016). Infiltration-excess overland flow to stream channels, as well as surficial mechanisms of RDI&I generation, may

be partially inhibited during warm seasons due to greatly enhanced interception and evaporation of precipitation from deciduous plant canopies (e.g., Xiao & McPherson, 2002). On average, our watersheds have 16% forest cover and much of that canopy coverage is by deciduous species.

The seasonality of GI is likely explained by seasonal changes in water-table elevation and prevailing hydraulic gradients within local aquifers (Figure S6 in the Supporting Information S1). Watersheds within the Piedmont province are largely underlain by crystalline metamorphic rocks and regolith that host unconfined aquifers. Over lengths of meters to tens of meters adjacent to stream channels the water-table surface may commonly fluctuate from less than one to over three m below land surface. Discharge from these unconfined, riparian aquifers contributes most of the flow within stream channels (Aulenbach & Peters, 2018; Peters & Aulenbach, 2011). Similarly, GI represents the majority fraction of total I&I as well (Figures 3 and 4). The water table maintains a relatively high elevation during cold, water-surplus seasons and descends to minimal elevations during warm, water-deficit seasons (Figure S6 in the Supporting Information S1). Groundwater infiltration is enhanced during the cold season because of the increased likelihood that the water table will intersect sanitary-sewer infrastructure across the entire network (Dirckx et al., 2016). Both GI and groundwater discharge to streams may also be enhanced during the cold season due to persistently steeper hydraulic gradients, which result from generally higher water-table elevations across the landscape but generally fixed elevations of stream channels and sanitary-sewer pipes.

The comparable seasonal dynamics of I&I and natural streamflow generation appear to result from common impacts associated with seasonal variations in soil wetness, groundwater storage within the landscape, and water-table elevation. Though seasonal fluctuations in I&I mirror those of natural streamflow generation, we reemphasize that I&I actually represents a diversion of meteorically derived water away from the local stream channel. The absolute volume of I&I diverted from local streamflow is therefore maximal during those times of year when streamflow is also maximal (Figures 4 and 5). However, the relative impact of I&I on local streamflow was generally greatest when streamflow magnitudes were lowest with Cobbs Creek watershed being an exception (Figure 8).

4.3. Variation in I&I Impacts on Streamflow Among Basins

The results in Figures 6 and 8 suggest that the impacts of I&I on streamflow can be divided into at least three qualitative patterns. Shoal Creek and Lower Snapfinger watersheds exemplify one pattern that is characterized by an accentuated impact across low flows. The potential impact on low-flow magnitudes associated with exceedance probabilities of 90%, 95%, and 99% is greater than the impacts on high flows (1%, 5%, and 10% exceedance probabilities) by a factor of three or more in each watershed. Doolittle Creek watershed exemplifies another pattern characterized by I&I impacts on streamflow that are more uniform across flows, though still more strongly accentuated for very low flows than very high flows. For example, the impact on very low flows (exceedance probability of 99%) is still greater by a factor of two or three than the impact on very high flows (exceedance probability of 1%). The impacts on low flows (90% and 95% exceedance probability) are still greater than the impact on the high flows (5% and 10% exceedance probability) but by less than a factor of two. In contrast to Shoal Creek and Lower Snapfinger watersheds, the 25th and 75th percentile flows are comparable for Doolittle Creek watershed. Finally, Cobb Creek watershed represents the sole case where the potential influence of I&I on streamflow was more pronounced among high flows than low flows.

There may be multiple reasons why different potential impacts of I&I on streamflow exist across these watersheds. The mechanisms of I&I generation may vary, for example, differences in timing of housing construction (and associated building codes) may yield spatial variability in the occurrence of downspout connections to sanitary-sewer systems. A higher frequency of this connection would significantly enhance rapid generation of RDI&I specifically during storm events, potentially enhancing the relative impact on high versus low flows in adjacent streams. The spatial variability in pipe and manhole defects could be another factor, which is likely related to construction materials and time since installation (e.g., Karpf & Krebs, 2011). The preferential occurrence of manhole flaws or pipe discontinuities in riparian zones or other topographic lows could enhance GI, whereas the preferential occurrence of these defects in upland areas may diminish GI, since the water table in those areas may be consistently deeper than the sanitary-sewer infrastructure. Or, it is conceivable that a similar magnitude of I&I across two watersheds may yield different relative impacts on high-flow versus low-flow magnitudes in streams if the temporal dynamics of streamflow vary between the same two watersheds. Exploring these hypotheses is beyond the scope of this paper but will be focal points in our subsequent research.

4.4. Sources of Remaining Uncertainty About the Impact of I&I on Streamflow

We acknowledge that some caution is warranted in the interpretation of data from Figures 7 and 8. These figures depict the potential change in streamflow that would occur if I&I were wholly abated. The results assume that all I&I would instead be directed to the local stream channel. It is possible that some portion of that flow (should I&I be abated) could be imbibed by the deep roots of trees and transpired to the atmosphere. In that case, the potential positive impact on streamflow would be smaller than we have shown. The likelihood of this alternative flow pathway is certainly lesser in urban than nonurban environments due to the considerably lower vegetation density and the prevalence of lawn grasses and ornamental plants whose root biomass exists predominantly above the water table. It is also known that urban soils have substantially higher densities than forested soils due to wheel and foot traffic, grading, and construction activities. These compacted soils are known to significantly reduce the depths of root penetration by trees (e.g., Bartens et al., 2009; Day & Bassuk, 1994; Day et al., 2000). Based on these facts, we would speculate that groundwater utilization by urban vegetation would only marginally impact the results shown in Figures 7 and 8.

The impact of I&I on local streamflow should also be considered with respect to other infrastructure-mediated flows in urban watersheds, some of which may have counteracting effects. One example is leakage of pressurized, potable water from conveyance pipes. If the potable water was sourced from an external basin (as is most, but not all, potable water delivered to users in the SRW), then that leakage represents an inflow term within the urban water balance along with precipitation. Some of that water could recharge local, unconfined aquifers and augment streamflow (e.g., Bhaskar et al., 2015; Lerner, 1986). Hence, some of the groundwater that is diverted away from the local stream channels via GI might be thought of as extraneous groundwater that only exists within the aquifer due to another infrastructure-mediated flow. To what degree this may be true in our basin is unknown. We have outlined a technical approach to investigate this question that we are initiating as part of a subsequent research project.

Exfiltration from the sanitary-sewer pipes into surrounding soil and saprolite could conceivably counteract reductions in streamflow that result due to GI. Any enhancement of streamflow by this process is not a desirable outcome, of course, because exfiltration may seriously pollute local aquifers and streams. The I&I impacts on streamflow we have reported may be positively biased due to our lack of quantification of exfiltration in Equations 4–6. When the water-table elevation falls below the fluid elevation in the pipe, then exfiltration of fluid from the pipe into the surrounding porous media can occur through some (though not all, for example, gutter downspouts and manhole walls) of the same defects that enable I&I. Exfiltration and I&I may be occurring simultaneously on different portions of the pipe system. Here, we briefly summarize evidence from existing studies, which suggests that exfiltration rates, and cumulative magnitudes, are relatively small in comparison to rates and totals of I&I.

Results from manipulative experiments and model simulations demonstrate a relatively low fraction of in-pipe flow that contributes to exfiltration across a range of flow conditions. Ellis et al. (2003) conducted manipulative experiments on defective pipe sections installed within recirculating flumes in a lab setting. Their results emphasize that paper waste and sediment within pipes can seal leaky joints and holes from the interior, resulting in 2- or 3-order-of-magnitude reductions in exfiltration rate relative to those observed for relatively clean water. They emphasize that these debris seals can be disrupted by very high and turbulent flows in the pipe (e.g., as induced by RDII) or by groundwater infiltration, thus explaining why the seals do not permanently inhibit I&I as well. Subsequent experiments on a different experimental system utilized actual sewage and demonstrated that the biological solids have a similar effect as sediment and paper debris, causing near complete sealing within one hour of radial pipe discontinuities ranging from 2 to 6 mm (Blackwood et al., 2005). In all experiments, the residual exfiltration rate following sealing was consistently less than 1% of the flow in the pipe (Blackwood et al., 2005). Karpf et al. (2011) simulated I&I and exfiltration during a 36-mm precipitation event over 12 hr for Dresden, Germany. Their model included fluid dynamics equations to simulate spatially distributed pipe flows and Darcy's Law to simulate water exchange between the pipes and surrounding porous media. Total I&I during the event exceeded approximately 1400 m^3 whereas total exfiltration was approximately 40 m^3. Hence, the magnitude of exfiltration was only about 3% of the magnitude of I&I. Overall, these studies provide a mechanistic understanding of why exfiltration rates should be lower than I&I along individual pipe lengths and approximations from model simulations that attempt to represent these mechanisms in their conceptualization and parameterization of an entire pipe network.

Estimates of exfiltration over longer time periods, and for whole watersheds, are almost entirely derived from model simulations or other water and/or solute mass-balance approaches (e.g., as reviewed by Nguyen et al., 2021). Nguyen and Venohr (2021) estimate that across Germany, 2.0%–2.1% of wastewater baseflow contributes to exfiltration. Based on results presented by Yang et al. (1999), Reynolds and Barrett (2003) infer that exfiltration may represent a similar percentage of wastewater baseflow (1.5%–2.0%) in Nottingham, UK. Reynolds and Barrett (2003) also summarize technical reports suggesting exfiltration could approach 6% of base wastewater flow in some German cities. For the sake of approximation, we assume that those previously reported values of exfiltration as a percentage of total wastewater flow (1%–6%; based on generally older sewers in European countries) are representative for our watersheds. We multiply the total, measured flow in the pipe over 2019 by those minimum and maximum percentages to yield cubic meters of exfiltration. Those volumes of exfiltration are divided by our estimated cumulative volumes of I&I over the same time to approximate the conceivable relative bias in those estimates. Assuming exfiltration is 1% of total wastewater flow, this calculation suggests that our I&I estimates for Cobbs, Doolittle, Lower Snapfinger, and Shoal Creek watersheds could be positively biased by 3.6%, 2.5%, 3.7%, and 4.0%, respectively. Assuming exfiltration is 6% of wastewater flow yields positive relative biases of 21.3%, 15.2%, 22.1%, and 24.1%, respectively.

This can only be considered a coarse bracketing of the plausible relative bias in our I&I estimates due to the unknown quantity of exfiltration occurring in the watersheds we studied. It is further complicated by the fact that some exfiltrating fluid may have actually entered the pipe system as RDII or GI. These uncertainties point to the imperative for more extensive monitoring of water-table dynamics in urban environments. Expanded observational capacity of water-table dynamics in urban watersheds would provide sorely needed data to verify what factions of sewer systems are, or are not, regularly inundated by groundwater, thus significantly aiding repair efforts. The same data would enable more rigorous calibration and verification of coupled pipe- and groundwater-hydraulic models that might be used to simulate I&I and exfiltration (e.g., as reviewed by Nguyen et al., 2021).

5. Conclusions

Inflow and infiltration of surface and groundwater into sanitary-sewer systems are pervasive in watersheds that receive significant precipitation and have shallow aquifers. Though recognized by engineers as a problem in the design and assessment of sanitary-sewer systems, the impact of I&I on urban streamflow regimes remains largely unknown. Our study of headwater basins within the Atlanta Metropolitan area, in combination with previous work from the Baltimore-Metropolitan area (Bhaskar et al., 2015; Bhaskar & Welty, 2012), suggests that I&I profoundly influences local streamflow regimes. As much as 24%–36% of the water in sanitary-sewer pipes within our study watersheds was freshwater of local meteoric origin, not wastewater. The largest fraction of that freshwater was groundwater. Returning that flow to the local stream channels could significantly enhance streamflow. The relative impact would be greatest on low flows that occur during short-term rainless periods and over summer and early fall seasons. Considering low flows associated with exceedance probabilities of 90%–99%, our results suggest that enhancements of as much as 6%–36% would be conceivable across all watersheds in this study. Enhanced monitoring of water-table dynamics in urban watersheds is identified as an imperative need for improved estimates of I&I and counteracting flows such as exfiltration. Additional research is needed to resolve mechanistic explanations for the variability of the impact of I&I on streamflow across urban and suburban watersheds.

Data Availability Statements

This research utilizes four time series of streamflow measured by the United States Geological Survey (USGS). The authors downloaded these data from the online, publicly available database administered by that agency. Any other person may obtain the data in the same way. This research utilizes four time series of precipitation and four time series of flow measured in sanitary sewer pipes. These data are publicly available from the DeKalb County Department of Watershed Management. The authors obtained these data by submitting an Open-Records-Request, which consists of a one-page form, specifying the desired data product that is submitted to that agency. Any other person may obtain the data in the same way. Data utilized in this project are publicly available from the noted federal and county agencies. The edited time series of streamflow, pipe flow, and precipitation used in this work are publicly available here: Pangle (2021).

Acknowledgments
We gratefully acknowledge funding support provided through the National Science Foundation Geography and Spatial Sciences Program via award NSF GSS 1853809. We thank the DeKalb County Department of Watershed Management for timely cooperation in addressing our open-record requests. We thank the three peer reviewers whose suggestions significantly improved this manuscript.

References

Abbott, B. W., Bishop, K., Zarnetske, J. P., Minaudo, C., Chapin, F. S., Krause, S., et al. (2019). Human domination of the global water cycle absent from depictions and perceptions. *Nature Geoscience*, *12*(7), 533–540. https://doi.org/10.1038/s41561-019-0374-y

Aulenbach, B. T., & Peters, N. E. (2018). Quantifying climate-related interactions in shallow and deep storage and evapotranspiration in a forested, seasonally water-limited watershed in the southeastern United States. *Water Resources Research*, *54*(4), 3037–3061. https://doi.org/10.1002/2017wr020964

Bach, P. M., Rauch, W., Mikkelsen, P. S., McCarthy, D. T., & Deletic, A. (2014). A critical review of integrated urban water modelling – urban drainage and beyond. *Environmental Modelling & Software*, *54*, 88–107. https://doi.org/10.1016/j.envsoft.2013.12.018

Bares, V., Stransky, D., & Sykora, P. (2009). Sewer infiltration/inflow: Long-term monitoring based on diurnal variation of pollutant mass flux. *Water Science and Technology*, *60*(1), 1–7. https://doi.org/10.2166/wst.2009.280

Bares, V., Stransky, D., & Sykora, P. (2012). Evaluation of sewer infiltration/inflow using COD mass flux method: Case study in Prague. *Water Science and Technology*, *66*(3), 673–680. https://doi.org/10.2166/wst.2012.229

Bartens, J., Day, S. D., Harris, J. R., Wynn, T. M., & Dove, J. E. (2009). Transpiration and root development of urban trees in structural soil stormwater reservoirs. *Environmental Management*, *44*(4), 646–657. https://doi.org/10.1007/s00267-009-9366-9

Beven, K., & Freer, J. (2001). Equifinality, data assimilation, and uncertainty estimation in mechanistic modelling of complex environmental systems using the GLUE methodology. *Journal of Hydrology*, *249*(1–4), 11–29. https://doi.org/10.1016/s0022-1694(01)00421-8

Bhaskar, A. S., & Welty, C. (2012). Water balances along an urban-to-rural gradient of metropolitan Baltimore, 2001–2009. *Environmental & Engineering Geoscience*, *18*(1), 37–50. https://doi.org/10.2113/gseegeosci.18.1.37

Bhaskar, A. S., & Welty, C. (2015). Analysis of subsurface storage and streamflow generation in urban watersheds. *Water Resources Research*, *51*(3), 1493–1513. https://doi.org/10.1002/2014wr015607

Bhaskar, A. S., Welty, C., Maxwell, R. M., & Miller, A. J. (2015). Untangling the effects of urban development on subsurface storage in Baltimore. *Water Resources Research*, *51*(2), 1158–1181. https://doi.org/10.1002/2014wr016039

Blackwood, D. J., Ellis, J. B., Revitt, D. M., & Gilmour, D. J. (2005). Factors influencing exfiltration processes in sewers. *Water Science and Technology*, *51*(2), 147–154. https://doi.org/10.2166/wst.2005.0042

Bonneau, J., Fletcher, T. D., Costelloe, J. F., & Burns, M. J. (2017). Stormwater infiltration and the 'urban karst' - A review. *Journal of Hydrology*, *552*, 141–150. https://doi.org/10.1016/j.jhydrol.2017.06.043

Burns, D. A. (2002). Stormflow-hydrograph separation based on isotopes: The thrill is gone - What's next? *Hydrological Processes*, *16*(7), 1515–1517. https://doi.org/10.1002/hyp.5008

Cahoon, L. B., & Hanke, M. H. (2017). Rainfall effects on inflow and infiltration in wastewater treatment systems in a coastal plain region. *Water Science and Technology*, *75*(8), 1909–1921. https://doi.org/10.2166/wst.2017.072

Cressler, C. W., Thurmond, C. J., & Hester, W. G. (1983). *Ground water in the greater Atlanta region* (Vol. 66). Georgia Geologic Survey Information Circular.

Day, S. D., & Bassuk, N. L. (1994). A review of the effects of soil compaction and amelioration treatments on landscape trees. *Journal of Arboriculture*, *20*(1), 9–17.

Day, S. D., Seiler, J. R., & Persaud, N. (2000). A comparison of root growth dynamics of silver maple and flowering dogwood in compacted soil at differing soil water contents. *Tree Physiology*, *20*(4), 257–263. https://doi.org/10.1093/treephys/20.4.257

Deen, A. R., Salbe, I., & Craig, R. W. (1992). Modelling of stormwater ingress into foulwater sewers. *paper presented at International Symposium on*. Urban Stormwater Management.

Diem, J. E., Hill, T. C., & Milligan, R. A. (2018). Diverse multi-decadal changes in streamflow within a rapidly urbanizing region. *Journal of Hydrology*, *556*, 61–71. https://doi.org/10.1016/j.jhydrol.2017.10.026

Diem, J. E., Pangle, L. A., Milligan, R. A., & Adams, E. A. (2021). Intra-annual variability of urban effects on streamflow. *Hydrological Processes*, *35*(9), e14371. https://doi.org/10.1002/hyp.14371

Dirckx, G., Bixio, D., Thoeye, C., De Gueldre, G., & Van De Steene, B. (2009). Dilution of sewage in Flanders mapped with mathematical and tracer methods. *Urban Water Journal*, *6*(2), 81–92. https://doi.org/10.1080/15730620802541615

Dirckx, G., Van Daele, S., & Hellinck, N. (2016). Groundwater Infiltration Potential (GWIP) as an aid to determining the cause of dilution of waste water. *Journal of Hydrology*, *542*, 474–486. https://doi.org/10.1016/j.jhydrol.2016.09.020

DWM. (2015). *System-wide flow and rainfall monitoring program* (p. 44). *Capacity, Management, Operations, and Maintenance*. DeKalb County Department of Watershed Management (DWMCMOM) Program.

Ellis, J. B., Revitt, D. M., Lister, P., Willgress, C., & Buckley, A. (2003). Experimental studies of sewer exfiltration. *Water Science and Technology*, *47*(4), 61–67. https://doi.org/10.2166/wst.2003.0221

EPA. (2004). *NPDES CSO report to congress*. Retrieved from https://www.epa.gov/npdes/2004-npdes-cso-report-congress

EPA. (2014). *Guide for estimating infiltration and inflow*. US Environmental Protection Agency Document. Retrieved from https://www3.epa.gov/region1/sso/pdfs/Guide4EstimatingInfiltrationInflow.pdf

Freer, J., McDonnell, J. J., Beven, K. J., Peters, N. E., Burns, D. A., Hooper, R. P., et al. (2002). The role of bedrock topography on subsurface storm flow. *Water Resources Research*, *38*(12), 5–1. https://doi.org/10.1029/2001wr000872

Karpf, C., Hoeft, S., Scheffer, C., Fuchs, L., & Krebs, P. (2011). Groundwater infiltration, surface water inflow and sewerage exfiltration considering hydrodynamic conditions in a sewer system. *Water Science and Technology*, *63*(9), 1841–1848. https://doi.org/10.2166/wst.2011.388

Karpf, C., & Krebs, P. (2011). Quantification of groundwater infiltration and surface water inflows in urban sewer networks based on a multiple model approach. *Water Research*, *45*(10), 3129–3136. https://doi.org/10.1016/j.watres.2011.03.022

Kaushal, S. S., & Belt, K. T. (2012). The urban watershed continuum: Evolving spatial and temporal dimensions. *Urban Ecosystems*, *15*(2), 409–435. https://doi.org/10.1007/s11252-012-0226-7

Konrad, C. E., & Fuhrmann, C. M. (2013). Climate of the southeast USA: Past, present, and future. In K. T. Ingram, K. Dow, L. Carter, & J. Anderson (Eds.), *Climate of the southeast United States: Variability, change, impacts, and vulnerability* (pp. 8–42). Island Press/Center for Resource Economics. https://doi.org/10.5822/978-1-61091-509-0_2

Kracht, O., Gresch, M., & Gujer, W. (2007). A stable isotope approach for the quantification of sewer infiltration. *Environmental Science & Technology*, *41*(16), 5839–5845. https://doi.org/10.1021/es062960c

Kracht, O., & Gujer, W. (2005). Quantification of infiltration into sewers based on time series of pollutant loads. *Water Science and Technology*, *52*(3), 209–218. https://doi.org/10.2166/wst.2005.0078

LeGrand, H. E. (1967). *Ground water of the piedmont and blue ridge provinces in the Southeastern states* (Vol. 538). United States Geological Survey Circular.

Lerner, D. N. (1986). Leaking pipes recharge groundwater. *Ground Water*, *5*, 654–662. https://doi.org/10.1111/j.1745-6584.1986.tb03714.x

Mein, R. G., & Apostolidis, N. (1992). A simple hydrologic model for sewer inflow/infiltration. *Paper presented at International Symposium on*. Urban Stormwater Management.
Mitchell, P. S., Stevens, P. L., & Nazaroff, A. (2007). Quantifying base infiltration in sewers: A comparison of methods and a simple empirical solution. In *Proceedings of the water environment federation* (pp. 219–238). https://doi.org/10.2175/193864707787974805
Mitchell, V. G. (2006). Applying integrated urban water management concepts: A review of Australian experience. *Environmental Management*, *37*(5), 589–605. https://doi.org/10.1007/s00267-004-0252-1
Mitchell, V. G., Cleugh, H. A., Grimmond, C. S. B., & Xu, J. (2008). Linking urban water balance and energy balance models to analyse urban design options. *Hydrological Processes*, *22*(16), 2891–2900, https://doi.org/10.1002/hyp.6868
Mitchell, V. G., Duncan, H., Inman, M., Rahilly, M., Stewart, J., Vieritz, A., et al. (2007). State of the art review of integrated urban water models. In *NOVATECH* (pp. 507–514).
Mitchell, V. G., McMahon, T. A., & Mein, R. G. (2003). Components of the total water balance of an urban catchment. *Environmental Management*, *32*(6), 735–746. https://doi.org/10.1007/s00267-003-2062-2
Mitchell, V. G., Mein, R. G., & McMahon, T. A. (2001). Modelling the urban water cycle. *Environmental Modelling & Software*, *16*(7), 615–629. https://doi.org/10.1016/S1364-8152(01)00029-9
Mittman, T., Band, L. E., Hwang, T., & Smith, M. L. (2012). Distributed hydrologic modeling in the suburban landscape: Assessing parameter transferability from gauged reference catchments. *Journal of the American Water Resources Association*, *48*(3), 546–557. https://doi.org/10.1111/j.1752-1688.2011.00636.x
Nguyen, H. H., Peche, A., & Venohr, M. (2021). Modelling of sewer exfiltration to groundwater in urban wastewater systems: A critical review. *Journal of Hydrology*, *596*, 126130. https://doi.org/10.1016/j.jhydrol.2021.126130
Nguyen, H. H., & Venohr, M. (2021). Harmonized assessment of nutrient pollution from urban systems including losses from sewer exfiltration: A case study in Germany. *Environmental Science and Pollution Research*, *28*(45), 63878–63893. https://doi.org/10.1007/s11356-021-12440-9
Pangle, L. (2021). Pangle_et_al_2022_streamflow_pipeflow_precipitation [Data set]. Mendeley Data, V1. https://doi.org/10.17632/f9vv593255.1
Pawlowski, C. W., Rhea, L., Shuster, W. D., & Barden, G. (2014). Some factors affecting inflow and infiltration from residential sources in a core urban area: Case study in a columbus, Ohio, neighborhood. *Journal of Hydraulic Engineering*, *140*(1), 105–114. https://doi.org/10.1061/(asce)hy.1943-7900.0000799
Peters, N. E., & Aulenbach, B. T. (2011). Water storage at the Panola mountain research watershed, Georgia, USA. *Hydrological Processes*, *25*(25), 3878–3889. https://doi.org/10.1002/hyp.8334
Rauch, W., Bertrand-Krajewski, J. L., Krebs, P., Mark, O., Schilling, W., Schutze, M., & Vanrolleghem, P. A. (2002). Deterministic modelling of integrated urban drainage systems. *Water Science and Technology*, *45*(3), 81–94. https://doi.org/10.2166/wst.2002.0059
Reynolds, J. H., & Barrett, M. H. (2003). A review of the effects of sewer leakage on groundwater quality. *Journal of the Chartered Institution of Water and Environmental Management*, *17*(1), 34–39. https://doi.org/10.1111/j.1747-6593.2003.tb00428.x
Soulsby, C., Birkel, C., & Tetzlaff, D. (2014). Assessing urbanization impacts on catchment transit times. *Geophysical Research Letters*, *41*(2), 442–448. https://doi.org/10.1002/2013gl058716
Trewartha, G. T., & Horn, L. H. (1980). *An introduction to climate*. McGraw-Hill.
U.S. Census Bureau. (2020). *Metropolitan and micropolitan statistical areas population totals and components of change: 2010–2019*. Retrieved from https://www.census.gov/data/tables/time-series/demo/popest/2010s-total-metro-and-micro-statistical-areas.html
Vazquez-Sune, E., Sanchez-Vila, X., & Carrera, J. (2005). Introductory review of specific factors influencing urban groundwater, an emerging branch of hydrogeology, with reference to Barcelona, Spain. *Hydrogeology Journal*, *13*(3), 522–533. https://doi.org/10.1007/s10040-004-0360-2
Voter, C. B., & Loheide, S. P. (2021). Climatic controls on the hydrologic effects of urban low impact development practices. *Environmental Research Letters*, *16*(6), 064021. https://doi.org/10.1088/1748-9326/abfc06
Walsh, C. J., Fletcher, T. D., & Burns, M. J. (2012). Urban stormwater runoff: A new class of environmental flow problem. *PLoS One*, *7*(9), e45814. https://doi.org/10.1371/journal.pone.0045814
Walsh, C. J., Roy, A. H., Feminella, J. W., Cottingham, P. D., Groffman, P. M., & Morgan, R. P. (2005). The urban stream syndrome: Current knowledge and the search for a cure. *Journal of the North American Benthological Society*, *24*(3), 706–723. https://doi.org/10.1899/04-028.1
Wittenberg, H., & Aksoy, H. (2010). Groundwater intrusion into leaky sewer systems. *Water Science and Technology*, *62*(1), 92–98. https://doi.org/10.2166/wst.2010.287
Wittenberg, H., & Brombach, H. (2002). Hydrologic determination of groundwater drainage by leaky sewer systems. In *Third international conference on water resources and environment research* (pp. 138–143).
Xiao, Q., & McPherson, E. G. (2002). Rainfall interception by Santa Monica's municipal urban forest. *Urban Ecosystems*, *6*(4), 291–302. https://doi.org/10.1023/b:Ueco.0000004828.05143.67
Yang, Y., Lerner, D. N., Barrett, M. H., & Tellam, J. H. (1999). Quantification of groundwater recharge in the city of Nottingham, UK. *Environmental Geology*, *38*(3), 183–198. https://doi.org/10.1007/s002540050414
Zhang, M. K., Liu, Y. C., Cheng, X., Zhu, D. Z., Shi, N. C., & Yuan, Z. G. (2018). Quantifying rainfall-derived inflow and infiltration in sanitary sewer systems based on conductivity monitoring. *Journal of Hydrology*, *558*, 174–183. https://doi.org/10.1016/j.jhydrol.2018.01.002
Zhang, M. K., Liu, Y. C., Dong, Q., Hong, Y., Huang, X., Shi, H. C., & Yuan, Z. G. (2018). Estimating rainfall-induced inflow and infiltration in a sanitary sewer system based on water quality modelling: Which parameter to use? *Environmental Science-Water Research & Technology*, *4*(3), 385–393. https://doi.org/10.1039/c7ew00371d
Zhang, Z. (2005). Flow data, inflow/infiltration ratio, and autoregressive error models. *Journal of Environmental Engineering*, *131*(3), 343–349. https://doi.org/10.1061/(asce)0733-9372(2005)131:3(343)
Zhang, Z. (2007). Estimating rain derived inflow and infiltration for rainfalls of varying characteristics. *Journal of Hydraulic Engineering-Asce*, *133*(1), 98–105. https://doi.org/10.1061/(asce)0733-9429(2007)133:1(98)
Zimmer, M. A., & McGlynn, B. L. (2017). Ephemeral and intermittent runoff generation processes in a low relief, highly weathered catchment. *Water Resources Research*, *53*(8), 7055–7077. https://doi.org/10.1002/2016wr019742